

Tagung Flachbodentanks  
Hamburg, 26.09.2019

**Low Cycle Fatigue of Shell-to-Base Joints in Storage Tanks during Operation**  
**Kurzzeitermüdung aus Betriebszuständen im Fußbereich von Lagertanks**  
**Knödel\*/Taras\*\*/Ummenhofer\*\*\***

\*Peter Knödel, Dr Knoedel Engineering Consultants, Baden-Baden, info@peterknoedel.de

\*\*Univ. Prof. Dr. techn. Andreas Taras, Professur für Stahlbau, Universität der Bundeswehr,  
München; ab 01.10.2019: o. Prof. für Stahl- und Verbundbau, ETH Zürich

\*\*\*Univ. Prof. Dr.-Ing. Thomas Ummenhofer, Lehrstuhl für Stahl- und Leichtbau, KIT Karlsruhe

**0 Contents**

0	<u>Contents</u>	1
1	<u>Introduction</u>	2
2	<u>Terms, Definitions and Abbreviations</u>	2
3	<u>Material Behaviour in Cyclic Loading</u>	3
4	<u>Filling Level Spectra (exemplary)</u>	6
4.1	General	6
4.2	Exemplary Oil Tanks Level Spectrum	7
4.3	Exemplary Fresh Water Tank Level Spectrum	9
5	<u>Exemplary Tank Design</u>	10
5.1	Geometry and Material	10
5.2	Characteristic Stress State – DBF	11
5.3	Plastic Strains at First Filling	13
5.4	Characteristic Stress State – FEA	14
6	<u>Welding Residual Stresses</u>	16
7	<u>Local Concepts</u>	17
8	<u>Conclusions</u>	18
9	<u>References</u>	19
9.1	Codes	19
9.2	Technical Literature	19

Dokument und Anhänge unterliegen dem Urheberrecht / Intellectual property rights reserved for this document and annexes

## 1 Introduction

Many flat bottom tanks of the oil industry have been built in the 1960s and 1970s, which are still in operation. Being usually designed for 25 years of operation, this time is by far exceeded. In this context it is discussed, if there could be a low cycle fatigue problem at the tanks bases.

In this paper investigate some aspects of low cycle fatigue with tank base joints are investigated.

## 2 Terms, Definitions and Abbreviations

CVG	cyclic void growth model only for $T \geq 1$ (see e.g. Häbig Fig. 2-24 [12])
DBF	design by formula (= “hand design”)
EC0, EC1, EC3, etc.	short form of EN 1990, EN 1991, EN 1993 [1], etc.
EDC	effective damage concept cannot predict failure for high-low loading history (see e.g. Häbig 2.4.7 [12])
FEA	finite element analysis
full filling cycle	full – empty – full (as opposite to full – partial empty – full)
hysteresis	characteristic stress-strain-curve of a material under cyclic loading with symmetric reversed strains (see Fig. 1)
isotropic hardening	only significant for strain reversal yield surface extends symmetrical to center (see e.g. Häbig Fig. 4-2 [12]) see kinematic hardening
kinematic hardening	only significant for strain reversal yield surface keeps size but shifts from centre (see e.g. Häbig Fig. 4-2 [12]) see isotropic hardening
ratcheting	progressive collapse when the loading is altered between two load levels (see Fig. 3)
SCF	stress concentration factor

Dokument und Anhänge unterliegen dem Urheberrecht / Intellectual property rights reserved for this document and annexes

shakedown	starting like a ratcheting phenomenon, but with decreasing strain amplitudes, so that a closed loop develops after e.g. 30 cycles [3] (see Fig. 3)
SWD	stress weighted damage model more accurate than CVG by including Lode angle to describe stress state more precisely (see e.g. Häbig 2.4.7 [12])
Triaxiality	$T = \sigma_{m,3} / \sigma_{v,3}$ (also denoted as triaxiality parameter $\eta$ , e.g. [4]) hydrostatic stress tensor / deviatoric stress tensor $\sigma_{m,3} = (\sigma_{1,3} + \sigma_{2,3} + \sigma_{3,3}) / 3$ $\sigma_{v,3} = \sqrt{(1/2) * [(\sigma_{1,3} - \sigma_{2,3})^2 + (\sigma_{2,3} - \sigma_{3,3})^2 + (\sigma_{3,3} - \sigma_{1,3})^2]}$ where $\sigma_{i,3}$ are principal stresses $T = 0$ pure shear (all components same magnitude) $T = \pm 1/6$ 3D – biaxial tension/compression $T = \pm 1/3$ 1D – tension/compression $T = \pm 2/3$ 2D – tension/compression $T \approx \pm 1$ 1D – tension/compression with blocking of lateral contraction $T = \pm \infty$ 3D – tension/compression
WRS	welding residual stresses
yield condition	after Hubert/Mises/Hencky describes a cylindrical yield surface

### **3 Material Behaviour in Cyclic Loading**

In the following figures some typical stress-strain-curves of plastic material behavior under cyclic loading are given.

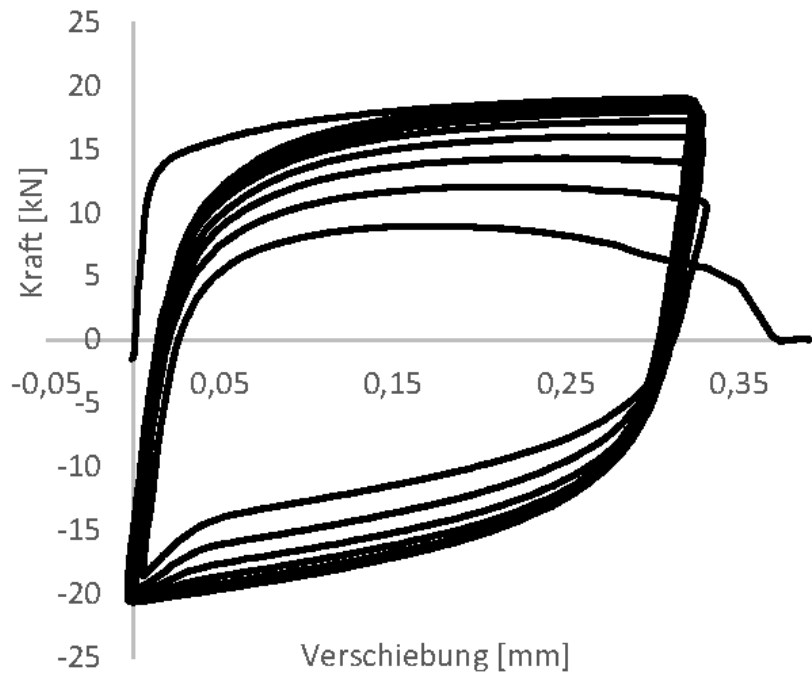


Figure 1: Closed Load-Elongation-Loops (hysteresis) under symmetric reversed strains up to gradual degradation during the last cycles and subsequent rupture (experimental data, Fig. 3-19 from [12])

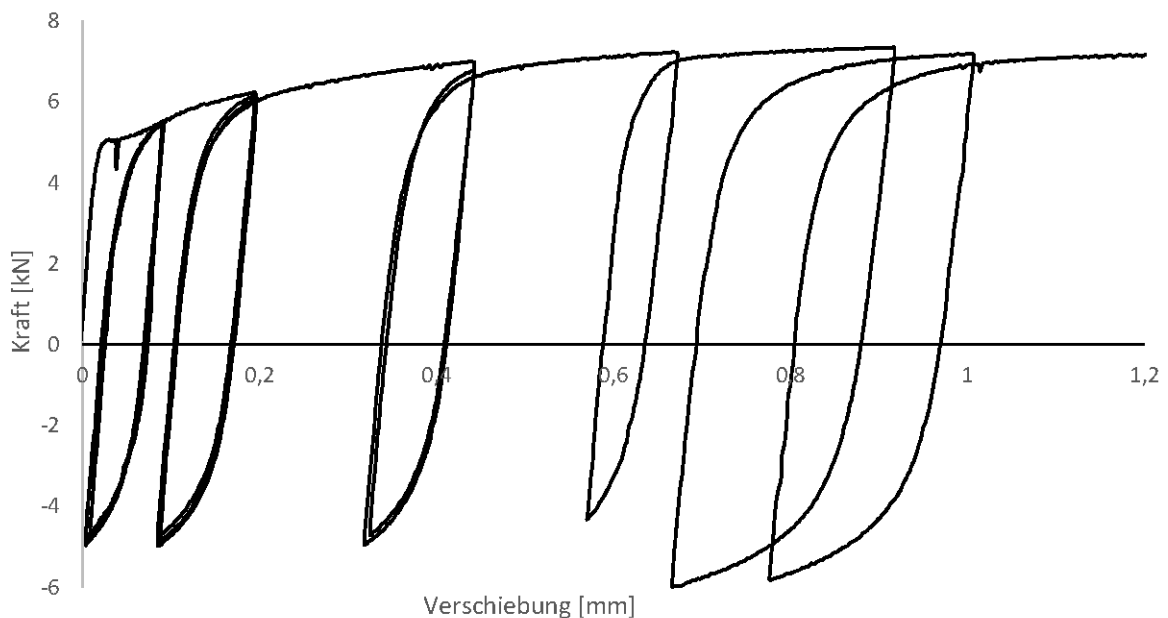


Figure 2: Open Load-Elongation-Loops under unsymmetric reversed strains (experimental data, Fig. 3-14 from [12])

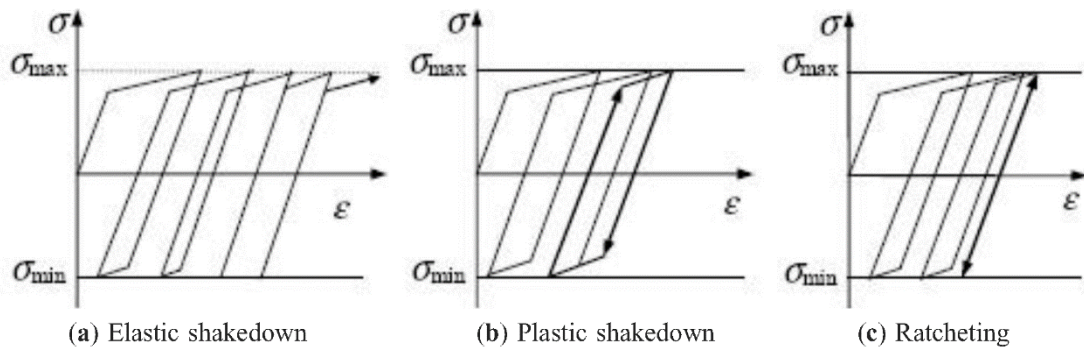


Figure 3: Sketches of shakedown and ratcheting (schematic, taken from [16])

The main differences of the plastic material behavior of a sample is coming from being load controlled (ratcheting or shakedown) or deformation controlled (open- or closed-loop hysteresis).

Another important feature comes from the fact, if after being plastified the load or deformation reversal is big enough to cause another plastification, which is associated with the term “Bauschinger-Effect” (see e.g. [9]). However, when there is a load or deformation reversal, but without plasticity (elastic unloading), neither of ratcheting or shakedown will happen (see Fig. 4).

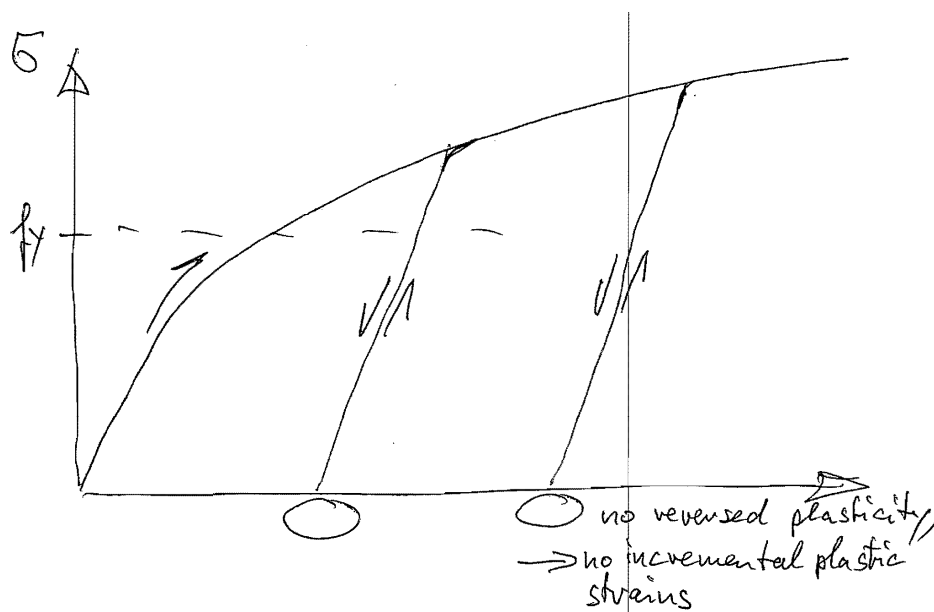


Figure 4: Sketch of repeated loading with elastic unloading

According to a hypothesis in material science, reversed plasticity takes place, if the unloading path is double the size of the yield limit. Other than sketched in Fig. 4, where a low yield limit is associated with high hardening potential, this is not the case for ordinary structural carbon steels. Thus, even if the tank should suffer plastic deformations during test filling, lowering the liquid level down

to zero will produce only elastic unloading without reversed plasticity. Consequently, subsequent filling will go up the elastic unloading path, but not produce any new plastic deformation.

When doing a “full” FEA, i.e. capturing fracture within the structural analysis, so called damage models are needed. These could be e.g. CVG, EDC, SWD, for a short explanations see the Terms and Definitions chapter. However, these are not used in the present study.

## **4 Filling Level Spectra (exemplary)**

### **4.1 General**

In order to tackle possible fatigue effects, information on the number of variations of stresses and the associated magnitudes are needed. In case of a tank, the circumferential membrane stresses, as well as the meridional bending stresses in the base joint area are proportional to the filling level of the stored liquid.

This first approximation assumption holds for ordinary tank design on basis of membrane stresses. It gets more complicated, if plastic deformations occur. These produce residual stresses after unloading (spring back), so that the resulting stress pattern – or more accurate: the resulting stress variations – are no longer proportional to the liquid level.

However, if not stated in more detail later in this paper, we will remain on this first approximation level. Thus, the stresses are proportional to the liquid level, and so are the stress variations. Therefore it is sufficient to provide a normalized filling level spectrum, which can be derived from the operators data. This normalized filling level spectrum holds also for the stress variations in the shell.

Although pretty many tank experts reject the idea of plastic tank design, Knödel, Ummenhofer and Ruckenbrod (2017) [14] showed, that this was an implicit part of tank design ever since.

Generally, tanks are not designed for spectrum loading. Rather, a tank has a specified nominal filling level, for which the quasi-static design is performed. Considering variations of load (i.e. emptying the tank and filling again), which could raise a fatigue issue (low cycle fatigue: LS2 acc. to EC3-1-6 [1] or high cycle fatigue LS4 acc. to EC3-1-6 [1]) is generally avoided by stating the number of load changes should not exceed 10.000.

For typical industrial vessels this seems to be a reasonable assumption. If you consider a design-lifetime of 25 years and one full filling cycle per day, you end up with 9.125 cycles. However, tanks

---

Dokument und Anhänge unterliegen dem Urheberrecht / Intellectual property rights reserved for this document and annexes

in the oil industry or in municipal fresh water supply, are much longer in operation, e.g. in excess of 50 years. Thus, arguing in favor of non-fatigue can only be done if

- a) the stress level is small  
which is not the case in typical tank design
- b) there is robust information on the number of filling cycles being still smaller than 10.000
- c) the total number of cycles is in excess of 10.000, but due to spectrum loading much of these cycles are not “full”, leading to a considerable longer design life than given by the SN-curve.

During the research for this paper we had support through the German and Austrian industry, which gave us the opportunity to present exemplary but real tank loading spectra, which we present in the subsequent subchapters.

## 4.2 Exemplary Oil Tanks Level Spectrum

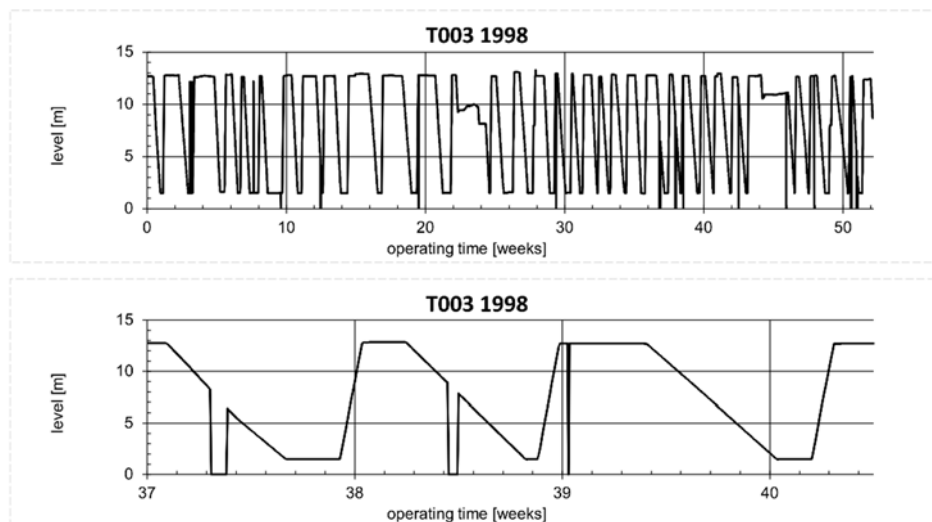


Figure 5. Example tank T3 – time history of filling level evaluated for 1998  
(courtesy of Bayernoil, Vohburg, Germany)

Tank 3 is a floating roof tank. It has a diameter of 51,20 m and an eaves height of 18,30 m. The nominal filling level of the tanks is app. 17,30 m.

In Fig. 5 we see 36 emptying cycles in 1998. Roughly, the level is alternating between 12,80 m and 1,50 m. A closer look to the drop downs to zero level in the bottom part of the figure shows, that these seem to be due to data error, because vertical lines would not match to the physical possibilities of the piping.

Thus we have a level range of

$$\Delta h = 12,80 \text{ m} - 1,50 \text{ m} = 11,30 \text{ m} \quad (1)$$

compared to a design level of 17,30 m.

From the frequency of emptying cycles we can conclude, that even if these were full cycles, the tank could have a service life of

$$N = 10.000 \text{ cycles} / 36 \text{ cycles/year} = 278 \text{ years} \quad (2)$$

to reach the magic number of 10.000 cycles.

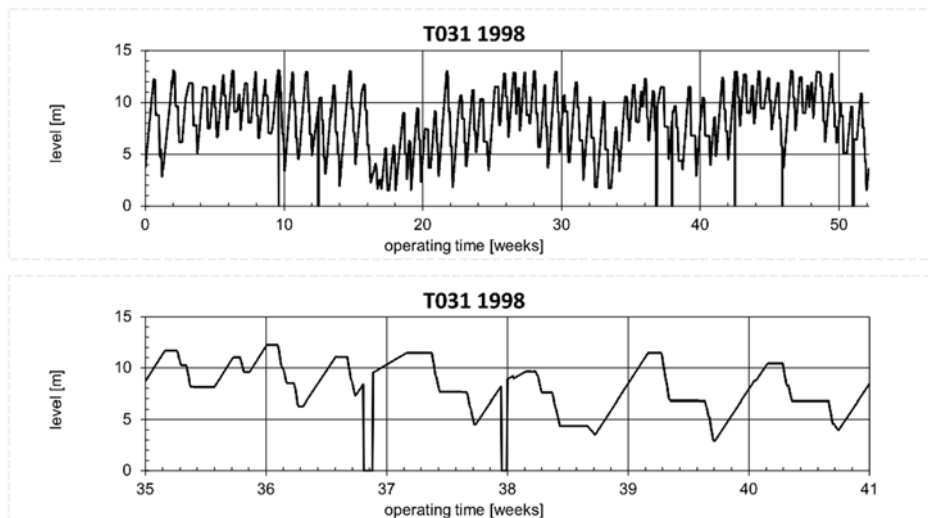


Figure 6. Example tank T31 – time history of filling level evaluated for 1998 (courtesy of Bayernoil, Vohburg, Germany)

Tank 31 has a diameter of 19,50 m and an eaves height of 18,30 m. Filling height at nominal volume is 18,10 m.

In Fig. 6 we see 63 emptying cycles in 1998. There is something like a long-time trend with app. 4 global waves along the year, which may be neglected in fatigue considerations. The remaining higher-frequency variations are having a range from app. 5 m (or smaller) to (not much more than) 8 m, compared to a design level of 18,10 m. If we exclude the range of > 5 m due to being insignificant for the loading spectrum, we have a regular (or “high-frequency”) variation of 5 m corresponding to 28 % of the nominal level.

Again, the drops down to zero level in the bottom part of the figure can be attributed to data error,

From the frequency of emptying cycles we can conclude, that even if these were full cycles, the tank could have a service life of

$$N = 10.000 \text{ cycles} / 63 \text{ cycles/year} = 159 \text{ years} \quad (3)$$

to reach the magic number of 10.000 cycles.

### 4.3 Exemplary Fresh Water Tank Level Spectrum

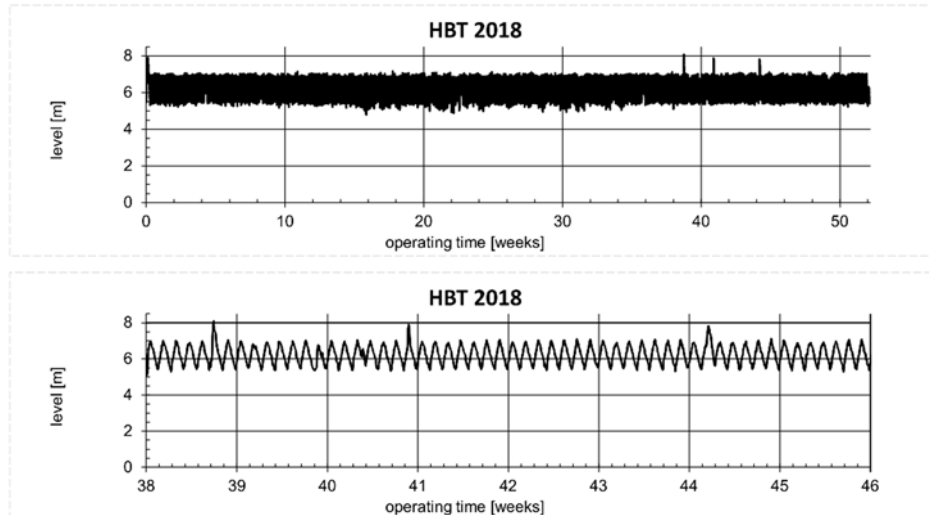


Figure 7. Example tank HBT – time history of filling level evaluated for 2018  
(courtesy of eww ag, Wels, Austria)

<<< HBT\_level-time-history\_2019-06-26\_a.tif >>>

HBT is a fresh water tank near Traunleiten, Austria, which is operated by the water department of Elektrizitätswerke Wels AG, Austria, since 2016/17. The structural analysis was done in 2016 by IPU Karlsruhe, Germany, with the first author being the structural engineer and the third author being owner of the design office.

The tank has diameter of 28.000 mm and an eaves height of 8.500 mm and a design filling height of 8.200 mm.

In Fig. 7 we see 56 emptying cycles during weeks 39-46 in 2018, i.e. 8 weeks. Mostly, a level between app. 5,50 m and app. 7,00 m is maintained, with rare peaks up to 8,00 m (only 4 throughout 2018). Thus, we have a range of app. 1,50 m with a frequency of 7 per week, making 1 per day or 365 per year.

This range of 1,50 m compares to the above given design level of 8,20 m, corresponding to 18 %.

From the frequency of emptying cycles we can conclude, that if these were full cycles, the tank could have a service life of

$$N = 10.000 \text{ cycles} / 365 \text{ cycles/year} = 27 \text{ years} \quad (4)$$

to reach the magic number of 10.000 cycles. It is obvious however, that due to the small actual level range (comparing to a small stress range), the tank can have a much longer service life.

## 5 Exemplary Tank Design

### 5.1 Geometry and Material

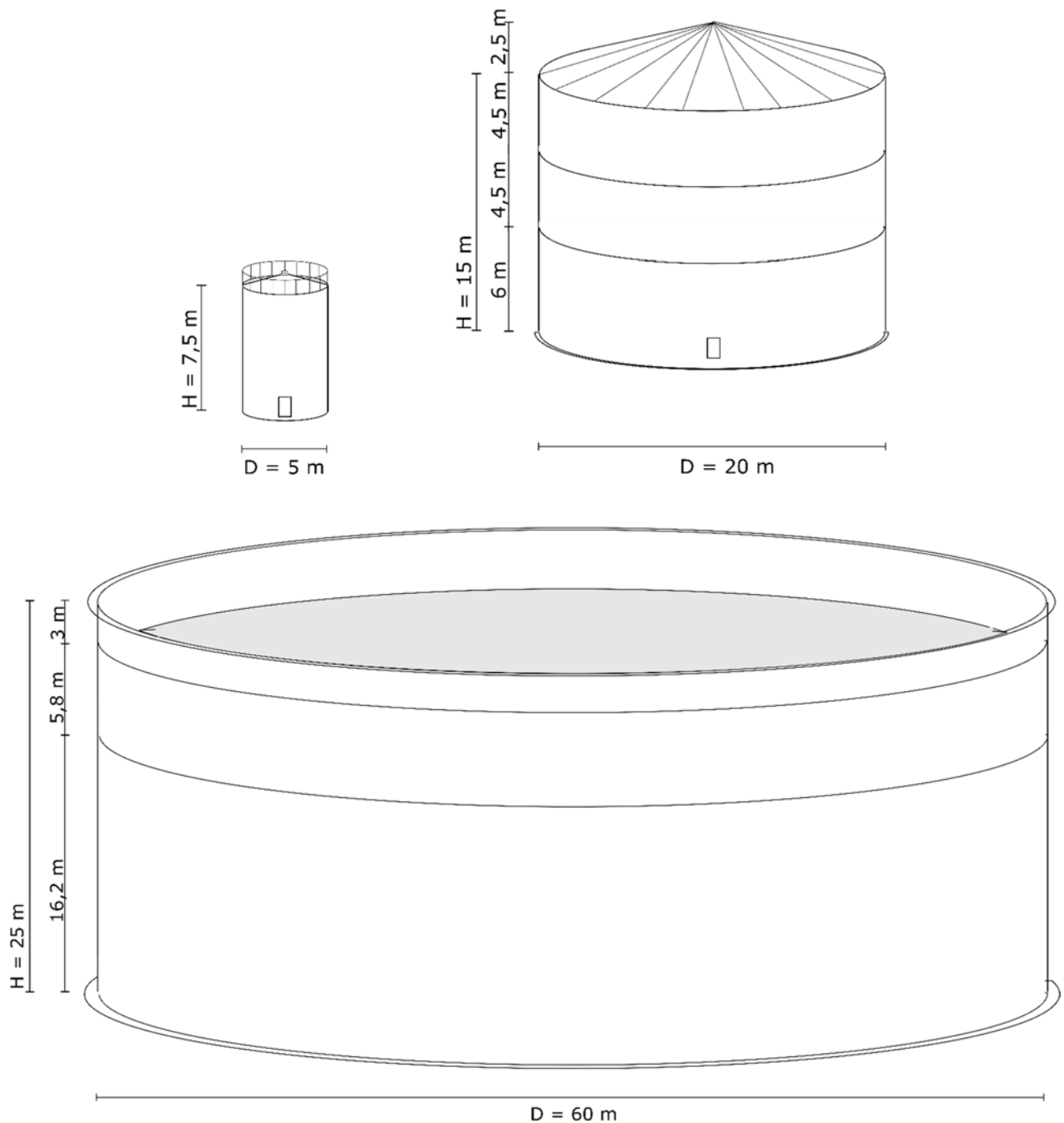


Figure 8. Three example tanks (not to scale), in [23])

We use a medium (20 m dia, 15 m eaves height, fixed roof) and a large tank (60 m dia, 25 m eaves height, floating roof), on which we worked within a research project for the German Building Authority DIBt (previously, these tanks were reported in [15]). Additionally, we use the Rüm-lang tank (Switzerland; 30 m dia, 26,3 m eaves height, fixed roof) given in [21], [22].

The stored liquid was considered to be water, operational filling level was at the eaves. Conventional membrane design according to EC3-4-2 [1] in comparison with DIN 4119 [2] gave the following results for the bottom strake:

medium tank

7,0 mm; S355;

large tank;

25,0 mm; S460;

Rüm-lang

15,5 mm; S355

this tank is operated with a liquid of  $8 \text{ kN/m}^3$ , but in the present study we use water as well

The constraints at the base joint are taken as

- bottom edge is radially fixed (zero-displacement condition)
- meridian of bottom edge is free to rotate (“pinned”) or alternatively rotation fixed (zero-tan-gent-inclination condition, “clamped”)

## 5.2 Characteristic Stress State – DBF

Characteristic values

medium tank:

$$\begin{aligned} & \text{hydrostatic pressure} && (5) \\ p &= 15 \text{ m} * 10 \text{ kN/m}^3 = 150 \text{ kN/m}^2 \\ & \text{membrane hoop stress according to Barlow's formula (“Kesselformel”)} \\ \sigma_{\phi} &= 150 \text{ kN/m}^2 * 10 \text{ m} / 7,0 \text{ mm} = 214 \text{ N/mm}^2 \\ & \text{safety margin to nominal yield limit} \\ S &= 355 \text{ N/mm}^2 / 214 \text{ N/mm}^2 = 1,66 \\ & \text{theoretical radial expansion} \\ \Delta R &= 10.000 \text{ mm} * 214 \text{ N/mm}^2 / 2,1 * 10^5 \text{ N/mm}^2 = 10,2 \text{ mm} \end{aligned}$$

large tank:

$$\begin{aligned} & \text{hydrostatic pressure} && (6) \\ p &= 25 \text{ m} * 10 \text{ kN/m}^3 = 250 \text{ kN/m}^2 \\ & \text{membrane hoop stress according to Barlow's formula ("Kesselformel")} \\ \sigma_{\varphi} &= 250 \text{ kN/m}^2 * 30 \text{ m} / 25,0 \text{ mm} = 300 \text{ N/mm}^2 \\ & \text{safety margin to nominal yield limit} \\ S &= 460 \text{ N/mm}^2 / 300 \text{ N/mm}^2 = 1,53 \\ & \text{theoretical radial expansion} \\ \Delta R &= 30.000 \text{ mm} * 300 \text{ N/mm}^2 / 2,1 * 10^5 \text{ N/mm}^2 = 42,9 \text{ mm} \end{aligned}$$

Rümlang tank

$$\begin{aligned} & \text{hydrostatic pressure} && (7) \\ p &= 26,3 \text{ m} * 10 \text{ kN/m}^3 = 263 \text{ kN/m}^2 \\ & \text{membrane hoop stress according to Barlow's formula ("Kesselformel")} \\ \sigma_{\varphi} &= 263 \text{ kN/m}^2 * 15 \text{ m} / 15,5 \text{ mm} = 255 \text{ N/mm}^2 \\ & \text{safety margin to nominal yield limit} \\ S &= 355 \text{ N/mm}^2 / 255 \text{ N/mm}^2 = 1,39 \\ & \text{theoretical radial expansion} \\ \Delta R &= 15.000 \text{ mm} * 255 \text{ N/mm}^2 / 2,1 * 10^5 \text{ N/mm}^2 = 18,2 \text{ mm} \end{aligned}$$

For the above mentioned constraints of the base joint, the resulting meridional bending stresses can be taken from EC3-1-6 Annex C [1] by means of a factor, which relates the meridional bending stresses to the circumferential hoop stresses.

clamped: 1,82

pinned: 0,585

Rümlang

$$\text{clamped: } \sigma_{x,b} = 1,82 * 255 \text{ N/mm}^2 = 464 \text{ N/mm}^2$$

$$\text{length of bending half-wave: } 2,44 * \sqrt{(R * T)} = 2,44 * \sqrt{(15.000 \text{ mm} * 15,5 \text{ mm})} = 1.178 \text{ mm}$$

to tackle the bending half wave in FE with linear elements this requires a maximum element length of  $1.178 \text{ mm} / 5 = 236 \text{ mm}$  (see Knödel/Ummenhofer/Ruckenbrod 2017 [14]), or, more modern,  $1.178 \text{ mm} / 10 = 118 \text{ mm}$

In order to capture the pronounced stress peak with a clamped bottom strake, we recommend to use the effective width with 5 elements:

---

Dokument und Anhänge unterliegen dem Urheberrecht / Intellectual property rights reserved for this document and annexes

$$0,778 * \sqrt{(R*T)} = 0,778 * \sqrt{(15.000 \text{ mm} * 15.5 \text{ mm})} = 375 \text{ mm},$$

thus  $375 \text{ mm} / 5 = 75 \text{ mm}$  (in this study we chose app. 50 mm)

With this element size we receive a maximum bending stress of  $-398 \text{ N/mm}^2$  at the base with an element size of app. 10 mm we receive  $-443 \text{ N/mm}^2$  at the base, which is still 5 % smaller than the analytical value.

### 5.3 Plastic Strains at First Filling

In conventional tank design (meaning hand design using formulae derived from structural mechanics) we cannot account for the flexibility of the tanks foot. Thus, doing design “on the safe side” we assume the tank’s foot to be clamped in order to get maximum meridional bending moments. If radial displacements would be an issue, we would alternatively assume a hinged tank’s foot in order to get maximum radial displacement of the tank’s wall.

The former assumption results in high meridional bending stresses which suggest yielding of the inner and outer surface of the tank’s wall. In a previous paper this effect has been discussed in detail. It was suggested that the a priory assumption of a plastic hinge around the tanks foot is beneficial, because it shortens the design process, still leading to safe results.

Another issue is the topic of partial safety factors. We are used from metal structures design, that we assume factorized loads on the action side, comparing these with the plastic (or stability) capacity of the component on the resistance side. From the perspective of reliability, the partial safety factor on the action can be seen as

- measure for the unlikely event of an actual load exceeding the nominal load;
- a number for controlling the probability of failure of the component (e.g. app. 1 over 1 million per year) within the given loading scenario;

As discussed only recently in the different Eurocode committees for load models (EC0 and EC1) and shell structures design (EC3-1-6 [1]), the liquid loads of a tank are far from being stochastic like e.g. wind loads. Rather, liquid levels (or filling volumes) are part of a controlled (industrial) process. Thus, we have close-to-deterministic loads, where even a partial load factor of e.g.  $\gamma_F = 1,2$  is over-conservative compared to the physical possibilities.

Therefore, when discussing plasticity and low cycle fatigue, the authors consider it simpler to refer to the nominal stress states. Only in an additional, second step we will look at what would happen, if the loads happen to be bigger than assumed in design.

---

Dokument und Anhänge unterliegen dem Urheberrecht / Intellectual property rights reserved for this document and annexes

## 5.4 Characteristic Stress State – FEA

Back to the question of realistic boundary conditions at a tank base. In a recent joint research project of the Universities Lausanne, Graz and Karlsruhe (KIT), low cycle fatigue at a tank base was investigated in the context of seismic loading. One of the outcomes was a PhD thesis of Tappauf (2018) [22] under the supervision of the second author, who was the project leader of the Graz' part. While this project was governed by highly dynamic response of the tank structure as well as by fully reversed loading, it is different with the present paper: looking only at operational conditions we have quasi-static loading, and we don't have load reversals. The question of possible strain reversals will be discussed later.

So we studied the quasi-static stress state under realistic boundary conditions, which implies the footplate lifting off the foundation. This was done by Zachmann (2019) in a Bachelor thesis [24]. Exemplary results are given in Fig. 9. As plausibility check we can see, that the maximum value for the radial displacement off the pinned model is short of 19 mm, which corresponds to the above analytical solution for the membrane state of 18,2 mm. As well we can see, that the circumferential membrane stress for the pinned model is short above 250 N/mm<sup>2</sup>, which corresponds to the above analytical solution for the membrane state of 255 N/mm<sup>2</sup>.

An interesting feature is seen with the comparison of the boundary conditions. In giving the bottom plate only vertical restraints to the foundation, it shows, that we have a radial displacement of some 4,5 mm, which is usually neglected in hand design. In turn, this leads to the fact, that the circumferential stresses are not going down to zero, as assumed in hand design, but remain at a value of app. 60 N/mm<sup>2</sup>. Still, the maximum values of radial displacements and membrane hoop stresses for the realistic boundary conditions are between the pinned and the clamped version, as would be expected.

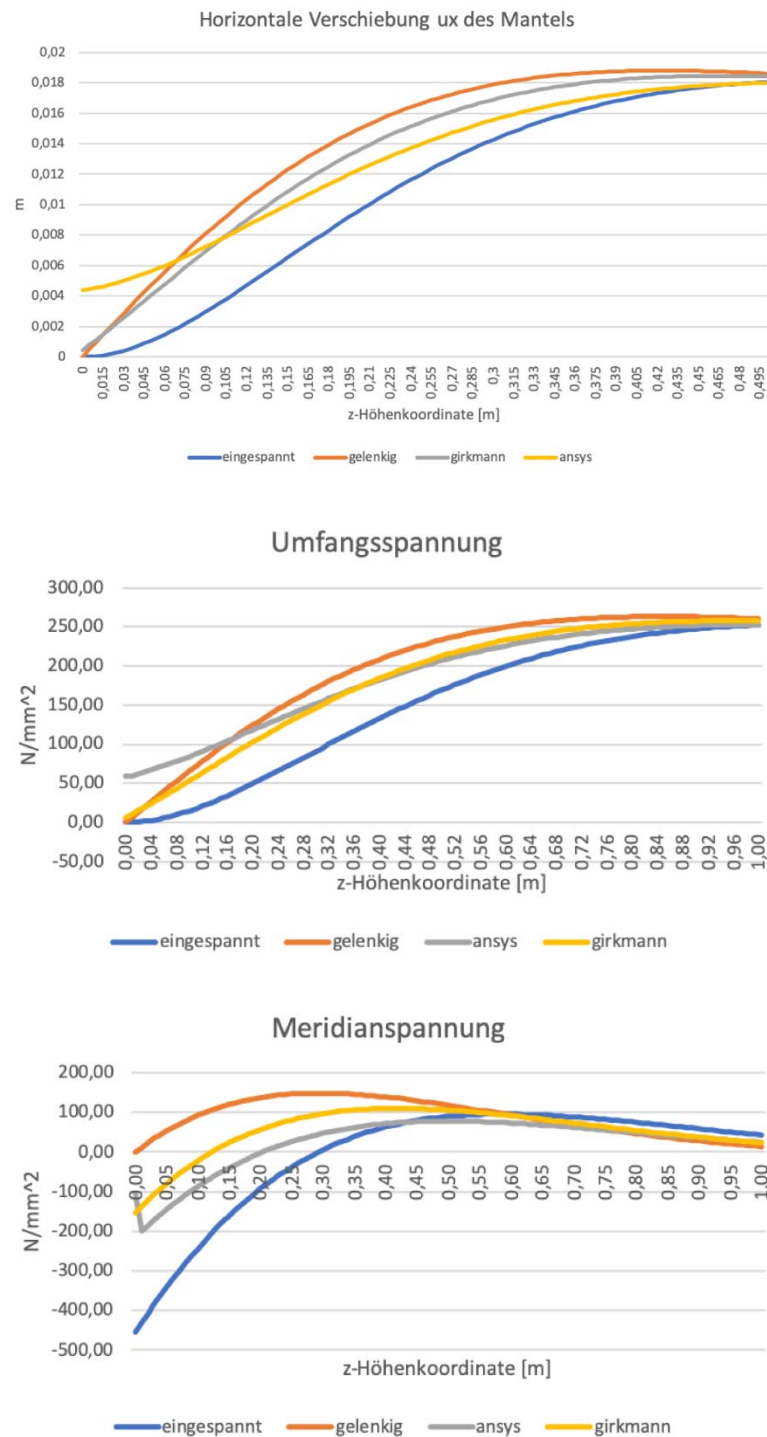


Figure 9: Rümlang Tank Base with different boundary conditions  
clamped (= eingespannt); pinned (= gelenkig); contact (= ansys); analytical (= girkmann [8])  
top: radial displacements; middle: circumferential membrane stress  
bottom: meridional bending stress (outer face of shell)  
(FEA, Fig. 2.17 from [24])

Also, as expected, the meridional bending stresses are between the pinned and the clamped version.

A value of 200 N/mm<sup>2</sup> compared to a clamped value of app. 450 N/mm<sup>2</sup> indicates, that the real

Dokument und Anhänge unterliegen dem Urheberrecht / Intellectual property rights reserved for this document and annexes

clamping moment at the base of the shell is less than half the value of an assumed clamped tank foot.

Minor variations are controlled by the activated stiffnesses, such as tank wall bottom strake and thickness of annular footplate. Also, the outstand of the footplate produces only a variation of the equivalent stresses in the tank wall from 100 N/mm<sup>2</sup> (75 mm outstand) to app. 50 N/mm<sup>2</sup> (0 mm outstand). We expected a higher influence of the outstand length. It seems however, that the lift of the inner part of the footplate, which is relaxing the shell wall's bending stresses is not very much dependent of the outstand length.

Thus we can assume, that these findings are also valid for anchored tanks, because the location of the anchors is typical well over 50 mm off the tank wall.

In his parametric study with a realistic parameter range, Zachmann did not find equivalent stresses bigger than 230 N/mm<sup>2</sup> in the tank wall or the foot plate of a tank with a reference hoop stress of 147 N/mm<sup>2</sup> [24]. For a rough estimate we can assume that the stress pattern of a tank with typical geometry of the base joint is such, that the equivalent stresses do not exceed the nominal circumferential membrane stresses by a factor of

$$k_{\text{est}} = 230 \text{ N/mm}^2 / 147 \text{ N/mm}^2 = \text{app. } 1,6 \quad (8)$$

## **6 Welding Residual Stresses**

Recently, Gkatzogiannis et al. are working on the FEA simulation of WRS (e.g. [10]).

The primary deteriorating effect of WRS is induction of high tensile stresses due to post-weld shrinkage. This corresponds to a mechanical prestressing of the weld area which, at cyclic loading, corresponds to an increase of the mean stress level.

Exemplary distributions of longitudinal and transverse WRS are given in Fig. 10. Basically, these can be compared with the situation at a tank base. As expected, longitudinal WRS are have the magnitude of the yield limit.

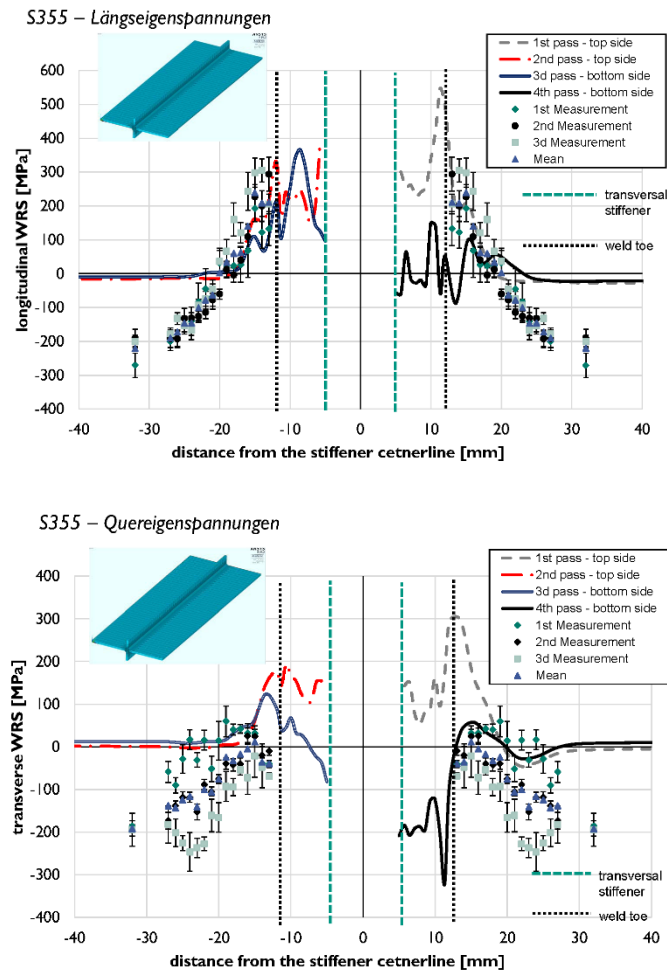


Figure 10: Longitudinal (top) and transverse (bottom) WRS FEA and measurements from [11]

## 7 Local Concepts

Other than nominal stress concepts in the previous chapter, which are dealing with mean stresses, local concepts are looking for actual hot spot stresses due to stress concentrations from variations in stiffness.

In the present component of a tank base we are looking of the SCF of a T-joint, where the “leg” is subjected to bending. This corresponds to EC3-1-9:2010 Table B1 Detail 7 [1], where a reference value of stress range of 90 MPa is given.

If the local stress state is known the evaluation of bearing capacity can be derived directly from the hysteretic material behavior.

This concept is mentioned here only for completeness, but will be not be investigated in further detail.

## **8 Conclusions**

Conclusions from the above results and discussions can be drawn as follows. Note, that these conclusions refer to operational states from variable filling levels in the tank, not to seismic loading.

- If tank walls are designed according to the present rules, the characteristic circumferential membrane stress is by a factor of 1,35 to 1,5 (or more) under the nominal yield limit.
- This factor will be smaller, if tanks would be designed by a deterministic approach, as proposed by Knödel/Ummenhofer 2018 [15].
- Due to meridional bending at the tank base, typically there will be equivalent stresses, which are by a factor 1,6 above the circumferential membrane stress.
- Due to the actual rotation of a tank base the clamping moment is reduced. The bending stresses are only half as much as calculated with the assumption of a clamped tank base.
- Along with residual stresses, there might be plastic deformations during first loading.
- In subsequent loading, no additional plastic strains will occur for two reasons:
  - a) there will be no filling level higher than first fill up to max;
  - b) due to the fact, that the hardening potential (relation of engineering ultimate stress and engineering yield stress) of structural steels is only app. 1,5, the stress range during unloading cannot be as much as  $2 f_y$ . Thus, no reversed plastic deformations can occur.
- From the previous bullet point follows, that all deformations within the service life of the tank will be elastic.
- The evaluation of realistic filling level spectra for medium to big tanks show, that either the tank has only very few emptying cycles, so that 10.000 cycles are not reached within the service life of the tank  
or the tank has frequent variations in the filling level, but only with a small range.

- Both cases of the previous bullet point let assume, that with an elaborate loading spectrum, a fatigue check for the tank can be done without being governing compared to the original design for static loads.

In summary we conclude, that flat bottom storage tanks, which have been built in the 1960s and 1970s, have no a priori low cycle fatigue problem due to the long service life. Of course, the above conclusions are based on the typical examples used. There might be a different situation when tanks having other filling histories.

Finally it should be noted, that in this study only the mechanical behavior of the Shell-to-Base Joints was studied. Inadequate corrosion protection might lead to shorter service life.

## 9 References

### 9.1 Codes

- [1] DIN EN 1993 Eurocode 3 (EC3): Design of steel structures. Part 1-6: Strength and stability of shell structures; German version EN 1993-1-6:2007 + AC:2009 + A1:2017. Juli 2017.
- [2] DIN 4119: Oberirdische zylindrische Flachboden-Tankbauwerke aus metallischen Werkstoffen. Above ground cylindrical flat bottom-tanks, constructed of metallic materials. Teil 1: Grundlagen, Ausführung, Prüfungen. Juni 1979. Part 1: General regulations, construction, tests. June 1979. Teil 2: Berechnung. Februar 1980. Part 2: Structural analysis and design. February 1980. Both parts withdrawn May 2011, at the same time the German NA to EC3-4-2 has been published.

### 9.2 Technical Literature

- [3] Agius, D., Wallbrink, C., Kourousis, K.I.: Cyclic Elastoplastic Performance of Aluminium 7075-T6 Under Strain- and Stress-Controlled Loading. JMEPEG 26 (2017) 5769-5780. doi.org/10.1007/s11665-017-3047-2
- [4] Bartsch, H.: Verification of damage mechanics approach to predict ductile failure of dissipative elements under seismic loading conditions (ULCF). Master Thesis, Institute of Steel Construction, RWTH Aachen, Prof. Dr.-Ing. M. Feldmann, September 2016.
- [5] Billur, E., Çetin, B., Uğuz, R.O., Davut, K., Arslan, E.: Advanced Material Characterization of TWIP Steels. pp. 303-317. Liewald, M. (ed.): New Developments in Sheet Metal Forming. Papers of the International Conferences on “New Developments in Sheet Metal Forming” and “New Developments in Hydroforming”, Fellbach, Germany 10+11 May 2016. TWIP = twinning induced plasticity, is an austenitic steel

- [6] Branco, R., Costa, J.D.M., Antunes, F.V., Perdigão, S.: Monotonic and Cyclic Behavior of DIN 34CrNiMo6 Tempered Alloy Steel. *Metals* 2016, 6, 98; pp. 1-14.  
<https://doi.org/10.3390/met6050098>
- [7] Desai, K.H., Joshi, D.C.; Predicting the Nonlinear Material Behaviour under Monotonic and Cyclic loading of SA333 and SS3304 Steels. *Int. Journal of Engineering Research and Application* (2016) Vol. 6, Issue 9, pp. 31-34.
- [8] Girkmann, K.: *Flächentragwerke*. Dritte Auflage, Springer, Wien 1954.
- [9] Gkatzogiannis, S., Knoedel, P., Ummenhofer, T.: FE welding residual stress simulation – Influence of boundary conditions and material models. Contribution 02\_02\_397 (USB) in [13].
- [10] Gkatzogiannis, S., Knoedel, P., Ummenhofer, T.: Simulation of Welding Residual Stresses – from Theory to Practice. Contribution ID 174. Proc., The 12th International Seminar “Numerical Analysis of Weldability”, 23-26 September 2018, Graz – Castle Seggau, Austria. P. 383-400 in Sommitsch, C., Enzinger, N., Mayr, P. (eds): *Mathematical Modelling of Weld Phenomena*. Verlag der Technischen Universität Graz, 2019.  
DOI 10.3217/978-3-85125-615-4-21
- [11] Gumbsch, P., Ummenhofer, T., Farajian, M., Knödel, P., Schubnell, J., Gkatzogiannis, S.; Rechnergestütztes Bewertungskonzept zum Nachweis der Lebensdauererlängerung von mit dem Hochfrequenz-Hämmerverfahren (HFMI) behandelten Schweißverbindungen aus hochfesten Stählen. Forschungsvorhaben der Forschungsvereinigung Schweißen und verwandte Verfahren e.V. des DVS, durchgeführt vom Fraunhofer Institut für Werkstoffmechanik (federführend) und von der Versuchsanstalt für Stahl, Holz & Steine, KIT, gefördert vom Bundesministerium für Wirtschaft und Energie (BMWi). Laufzeit vom 01.01.2017 bis zum 30.06.2019, verlängert bis 31.12.2019.
- [12] Häbig, M.: Versuchstechnische Bestimmung und numerische Evaluierung von Werkstoffparametern für die Anwendung in plastischen Schädigungsmodellen. Determination and numerical evaluation of material parameters for use in plastic damage models. Master Thesis with Prof. Dr.-Ing. T. Ummenhofer, KIT Steel & Lightweight Structures, Karlsruhe 2016.
- [13] Jönsson, J.: Proceedings, Eurosteel 2017, 8th European Conference on Steel and Composite Structures. 13-15 September 2017, Copenhagen, Denmark. ce/papers 1 (2017), Issue 1, September 2017.
- [14] Knödel, P., Ummenhofer, T., Ruckenbrod, C.: Silos und Tanks. Kap. 10, S. 595-692 in Kuhlmann, U. (Hrsg.): *Stahlbau Kalender 2017*, Ernst & Sohn, Berlin.
- [15] Knödel, P., Ummenhofer, T.: Remarks on the Safety Concept of Tank Structures. Anmerkungen zum Sicherheitskonzept von Tankbauwerken. 11<sup>th</sup> Conference on Flat Bottom Storage Tanks, 17-18 October 2018, Munich, Germany.
- [16] Mouattah, K., Bali, A.: Prediction of structural ratcheting by various models. *Materials at High Temperatures* 28(1), 21-27 (2011).  
doi: 10.3184/096034011X12962347725684
- [17] Nagel, S., Knödel, P., Ummenhofer, T.: Testing of Ultra-Low Cycle Fatigue at Complex Loading Scenarios. 2nd International Conference on Structural Integrity, ICSI 2017, 4-7 September 2017, Funchal, Madeira, Portugal. *Procedia Structural Integrity* 5 (2017), pp 1377-1384.

- [18] Nagel, S., Knödel, P.: Ultrakurzzeitfestigkeit von geschweißten Verbindungen unter mehrachsigen Beanspruchungszuständen. 21. DAST-Forschungskolloquium, 06.-07.03.2018, TU Kaiserslautern.
- [19] Papadrakakis, M., Fragiadakis, M. (eds): Proc. COMPDYN 2017, 6<sup>th</sup> ECCOMAS Thematic Conference on Computational Methods in Structural Dynamics and Earthquake Engineering, 15-17 June 2017, Rhodes Island, Greece.
- [20] Schaffrath, S., Bartsch, H., Hoffmeister, B., Feldmann, M.: Prediction of Ductile Damage in case of Seismic Action using innovative Damage Mechanics. P. 4496-4508 in c.
- [21] Tappauf, C., Taras, A.: Deformation and Strain Histories in Shell-to-Base Joints of Unanchored Steel Storage-Tanks during Seismic Loading. 8<sup>th</sup> Int. Conf. on Behavior of Steel Structures in Seismic Areas, Shanghai, China, July 1-3, 2015.
- [22] Tappauf, C.: Ermüdungsverhalten von unverankerten Stahltanks bei Erdbeben. Dissertation, TU Graz, Juni 2018. (Fatigue behaviour of un-anchored steel tanks with earthquake, PhD)
- [23] Ummenhofer, T., Knödel, P., Nagel, S.: Vergleichsberechnungen zu stehenden, zylindrischen, standortgefertigten, drucklosen Behältern nach DIN EN 1993-4-2 / DIN 4119. Kurztitel: Vergleichsberechnungen zu stehenden zylindrischen Tankbauwerken. Forschungsprojekt Nr. 161502 an der Versuchsanstalt für Stahl, Holz und Steine, KIT Karlsruhe. Gefördert vom DIBt, Geschäftszeichen P52-5-19.82-1996/16. Abschlussbericht vom 05.08.2018. (Comparative calculations on vertical, cylindrical site built, unpressurized tanks according to DIN EN 1993-4-2 / DIN 4119)
- [24] Zachmann, A.: Untersuchungen zu plastischen Zonen im Fußbereich von Tanks. A Study on Plastic Zones of Shell-to-Base Joints in Storage Tanks. Bachelor Thesis at KIT Steel and Lightweight Structures, Univ.-Prof. Dr.-Ing T. Ummenhofer, August 2019.